Supplementary Methods

Retrovirus infection and Screen for P10NRGLs. Retrovirus infection was performed as we have previously described (58). pLIB-based retroviral cDNA library (2-3 $x10^6$ individual clones) derived from normal human prostate was purchased from Clontech. The library was amplified once. pLIB vector and the cDNA retrovirus were prepared as described (58). LNCaP cells, 1-$2x10^5$ in a 100mm dish seeded one day earlier, were infected with pLIB or cDNA library retrovirus for 48 hours and then infected with pBabe-PTEN for 48 hours. pLIB contains no antibiotic selection marker. The cells were selected in puromycin at 1 μg/ml for PTEN infection for three weeks until the surviving cell colonies formed. Based on a LacZ reporter retrovirus, at least 70% of LNCaP cells were infected (data not shown).

Identification of candidate cDNAs. Genomic DNA was purified from single surviving cell colonies. Exogenous PTEN was confirmed by PCR using a pair of primers (forward primer 5'-CAT AAC CCA CCA CAG CTA GAA CT-3'; reverse primer 5'-ATC ACC ACA CAC AGG CAA TGG-3') for 35 cycles at 94°C for 45 seconds, 55°C for 45 seconds, and 72°C for 45 seconds. The genomic DNA from PTEN positive surviving cells was subjected to PCR amplification using a pair of primers specific for pLIB (forward primer 5'-CGG GAT CCA GCC CTC ACT CCT TCT CTA G-3'; reverse primer 5'-CGG AAT TCC TAC AGG TGG GGT CTT TCA TT-3'). The PCR conditions were 95°C for 10 minutes, 5 cycles of 95°C (45 seconds)-60°C (45 seconds)-72°C (1 minute), 35 cycles of 95°C (45 seconds)-65°C (45 seconds)-72°C (1 minute), and 72°C for 15 minutes. The PCR products were subcloned into a TA-cloning vector, followed by sequence determination.

One of candidates sequenced encoded a C-terminal SIPL1 fragment containing residues 225 – 387 (full length SIPL1 consists of 387 amino acid residues, see Figure 4E). This fragment encompasses the ubiquitin-like domain (UBL) between residues 240 – 300 (Supplementary Figure 1D). Although this fragment does not have the translation initiation codon (ATG), the upstream linker, used to construct the cDNA library, provided the initiation codon ATG and six additional residues (MAAAAST).

Supplementary video 1. Co-localization of endogenous PTEN (red) with endogenous SIPL1 (green) in MCF7 cells. MCF7 cells were IF stained for PTEN (red) and MAN2C1 (green). Nuclei were counterstained with DAPI (blue). Z-stack images were acquired using a MP Leica TCS SP5 confocal microscope and 3-D video was reconstructed using the IMARIS software (Biopane Inc).

Supplementary Figure 1

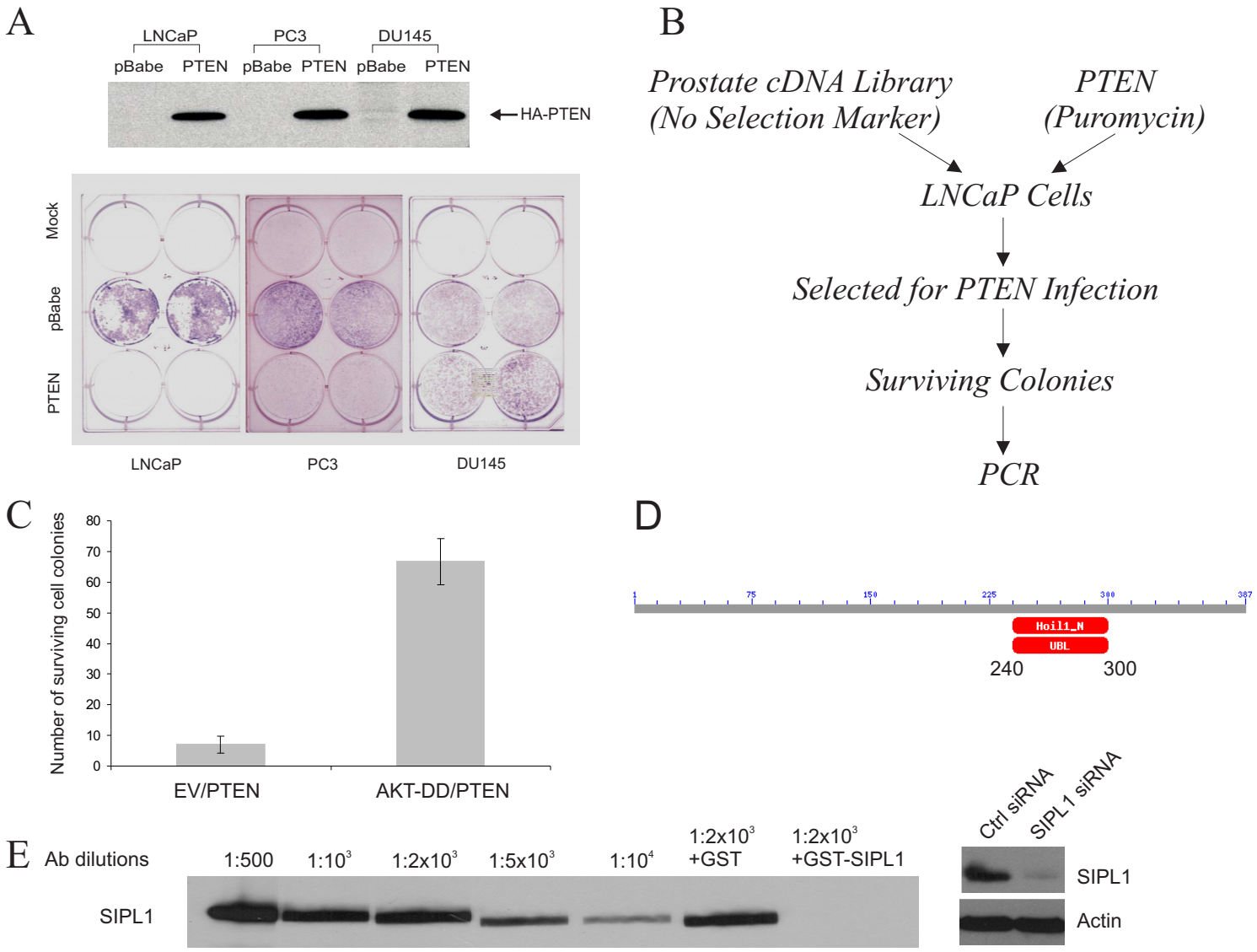

Supplementary Figure 1. Identification of SIPL1 as a PTEN-NR. (**A**) PTEN potently inhibits LNCaP cell proliferation. LNCaP, PC3, and DU145 prostate cancer cells were left untreated (mock) or infected with either an empty vector (pBabe) or PTEN retrovirus. Expression of HA-tagged PTEN was confirmed (top panel). The cells were selected in puromycin and viable cells were stained in 0.1% crystal violet (bottom panel). (**B**) A strategy for screening for PTEN negative regulators (PTEN-NRs). LNCaP cells were infected with a prostate cDNA library and PTEN retrovirus, followed by selection for PTEN infection with puromycin. Ectopic PTEN potently inhibited LNCaP cell growth, which was attenuated by cDNAs encoding PTEN-NRs. These cDNAs were subsequently amplified from genomic DNA isolated from surviving cells by PCR using a pair of primers matched to the cloning sites used to construct the cDNA library. (**C**) LNCaP cells were infected with pBabe (empty vector: EV)/PTEN or AKT-DD/PTEN. Expression of ectopic PTEN and AKT-DD was confirmed (data not shown). Surviving cells were stained and quantified. Experiment was repeated at least three times. (**D**) A cDNA encoding residues 225-387 of SIPL1 was obtained from our screen. GeneBank BLAST search revealed that this fragment contains a Hoil_N homologue domain or UBL (ubiquitin like) domain. (**E**) Anti-SIPL1 antibody was raised, purified, and used at the indicated dilutions to examine endogenous SIPL1 protein in DU145 cells by western blot. The antibody at 1:2000 dilution detected SIPL1 in DU145 cells in the presence of GST but not GST- SIPL1. Note: a single western blot membrane was cut into strips for the indicated western blot and strips were placed together for film exposure (left panel). DU145 cells were treated with Ctrl siRNA or SIPL1 siRNA, followed by western blot analysis for actin and SIPL1 using our anti-SIPL1 antibody (right panel).

Supplementary Figure 2

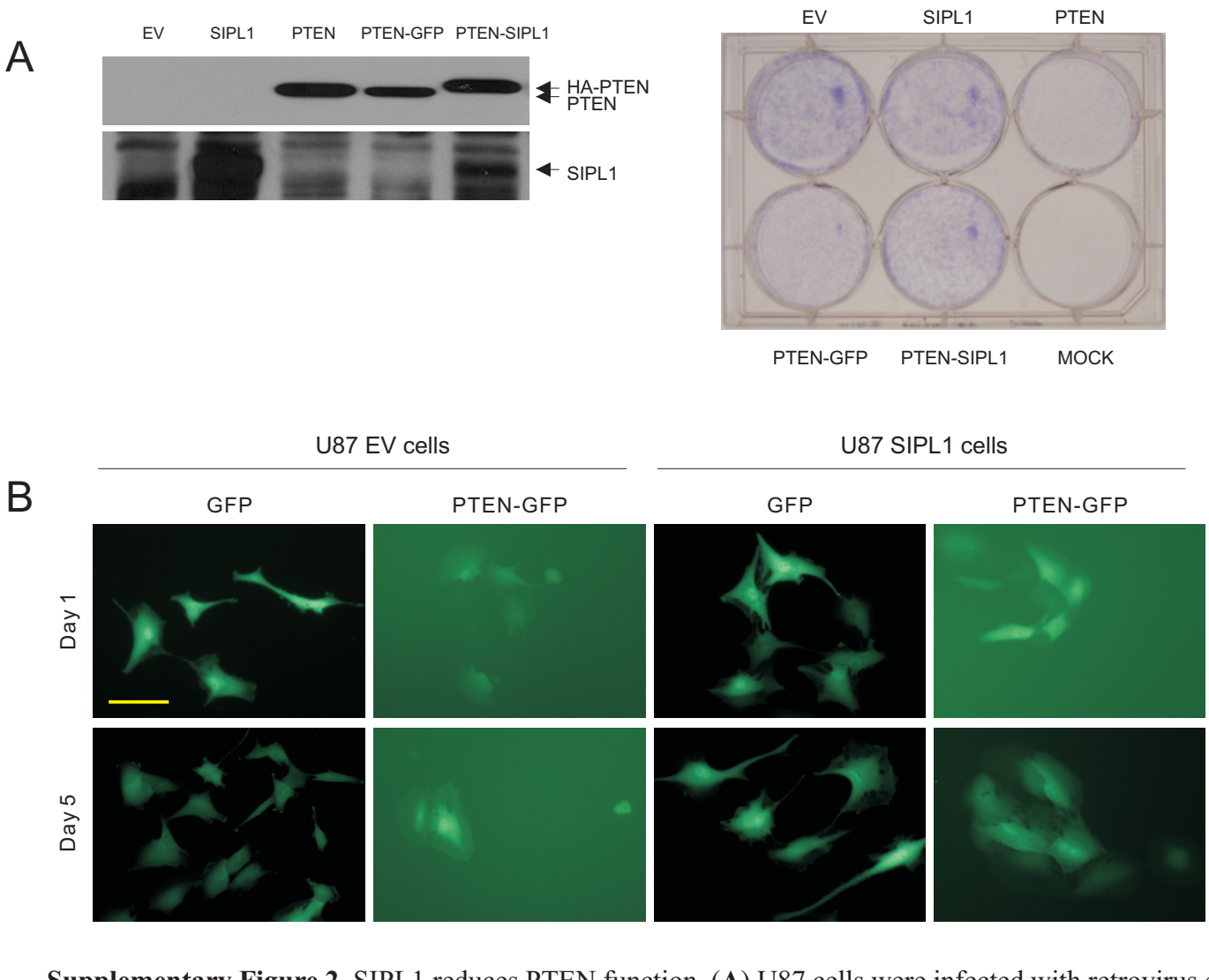

Supplementary Figure 2. SIPL1 reduces PTEN function. (**A**) U87 cells were infected with retrovirus expressing empty vector (EV), SIPL1, PTEN, PTEN-IRES-GFP (PTEN-GFP), and PTEN-IRES-SIPL1 (PTEN-SIPL1; IRES: internal ribosome entry site). Expression of individual ectopic proteins was demonstrated (left panel). Infected cells were cultured in medium supplemented with hygromycin for 2-3 weeks and surviving colonies were stained with crystal violet (right panel). Mock: cells were treated without retroviral infection and selected in hygromycin-containing medium. Experiments were carried out three times. (**B**) U87 cells stably expressing EV and SIPL1 were infected with either GFP or PTEN-IRES-GFP (PTEN-GFP) retrovirus. Approximately 90% of cells were GFP-positive 24 hours after viral infection. Apoptotic cells were clearly detected in PTEN-GFP infected U87 EV cells. GFP-positive cells sharply declined in U87 EV cells infected with PTEN-GFP with or without addition of hygromycin, when compared to other infections. At day 5, approximately 10% of GFP-positive cells in the PTEN-GFP infected U87 EV cells remained (most of them being apoptotic), while 50 – 60% of GFP-positive PTEN-GFP U87 SIPL1 cells were viable. Typical morphological images at day 1 and 5 were shown. For clarity, images shown here were derived from cells using hygromycin from day 2 onward. Images were taken using autoexposure. The high levels of background in cells infected with PTEN-GFP were a consequence of the microscope settings necessary to detect the low levels of GFP when driven by IRES as compared to GFP virus infected cells (driven directly by a CMV promoter). Scale bar: 50 μm.

Supplementary Figure 3

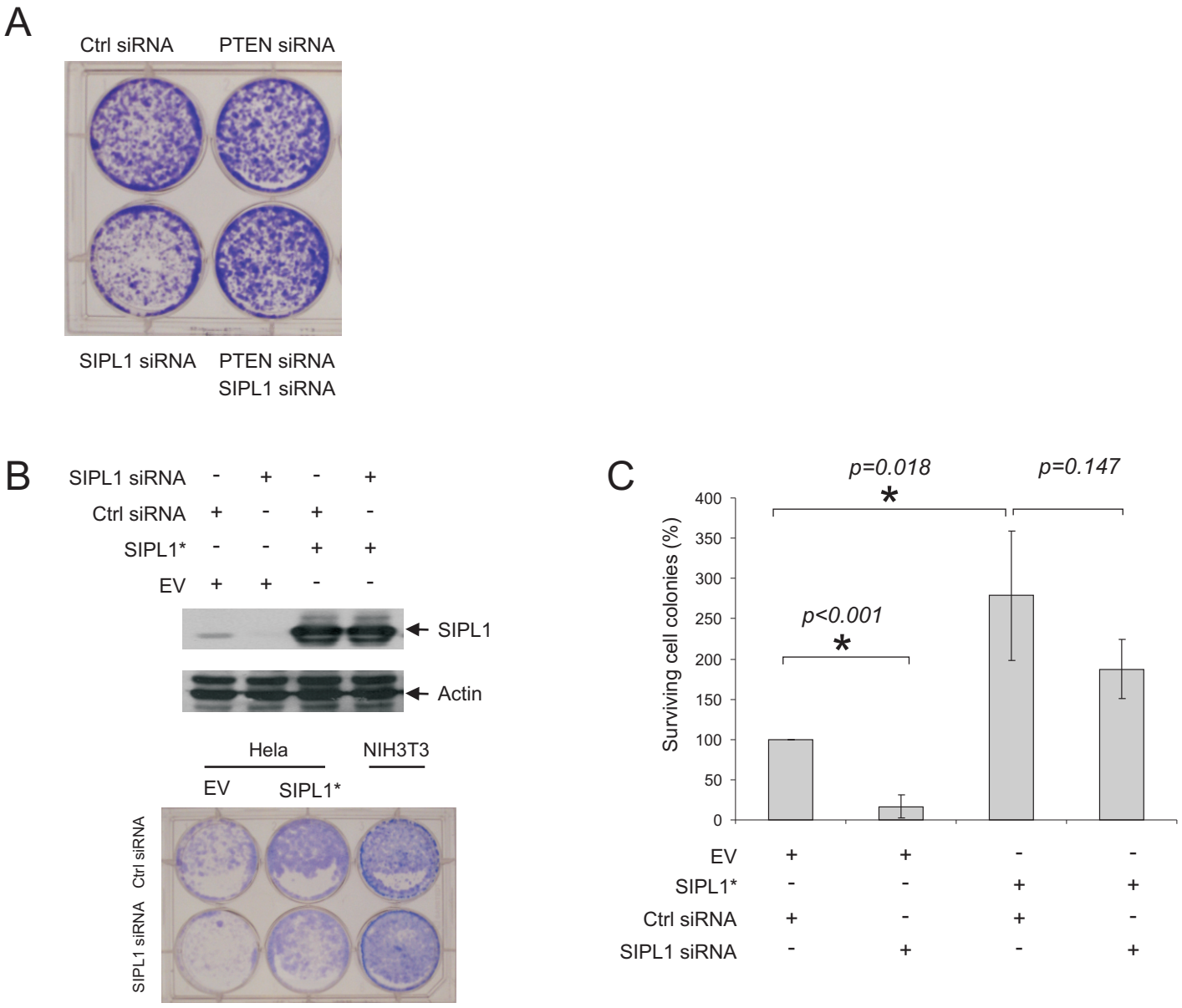

Supplementary Figure 3. Knockdown of SIPL1 reduces cell growth by activating endogenous PTEN function. (**A**) DU145 cells were infected with the indicated retrovirus. Knockdown of individual proteins was demonstrated (data not shown). Infected cells were selected in puromycin-containing medium. Surviving cell colonies were stained. (**B**) HeLa cells were infected with an empty vector (EV) or siRNA resistant SIPL1* which was generated by substituting the siRNA targeting sites but maintaining the amino acid identities. SIPL1 expression was examined by western blot (top panel). HeLa and NIH3T3 cells were infected with the indicated retrovirus and selected with hygromycin for 2 days. Surviving cells were stained with 0.1% crystal violet. As SIPL1 siRNA was human specific, murine NIH3T3 cells were used to show comparable titers between Ctrl siRNA and SIPL1 siRNA retrovirus. (**C**) The numbers of surviving cell colonies were analyzed using the Image-J software and expressed as the percentages of their respective empty vector treated cells.

Supplementary Figure 4

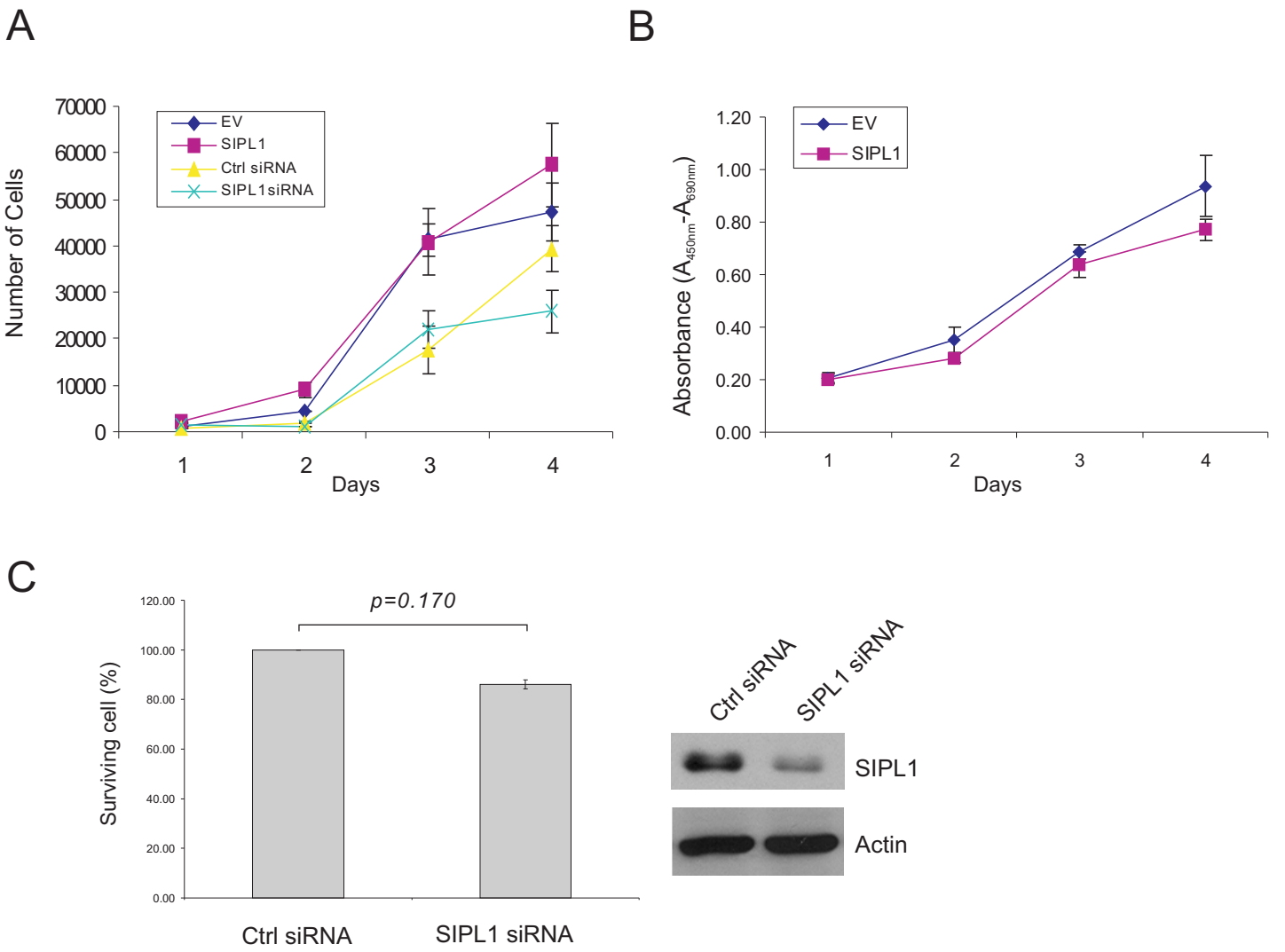

Supplementary Figure 4. Modulation of SIPL1 expression did not affect the growth of PTEN deficient cells. (**A**) U87 and (**B**) C33A cells were stably infected with EV or SIPL1 retrovirus, followed by determination of cell proliferation by counting cell numbers daily (A) or using the WST-1 cell proliferation kit (Clontech, according to the manufacturer's instructions) (B). U87 (**A**) and LNCaP (**C**) cells were treated with a Ctrl siRNA or SIPL1 siRNA, followed by examination of cell proliferation curves (A) or colony formation capacity (C). In brief, colony formation assay was carried out by seeding 10^3 cells per 6-well in triplicates. Cells were cultured for 2 weeks. Surviving colonies were stained and analyzed using the Image-J software. Statistical analysis of the growth characteritics observed between EV and SIPL1 cells, as well as between Ctrl siRNA and SIPL1 siRNA cells, in panels A, B, and C showed no significant difference ($p > 0.05$).

Supplementary Figure 5

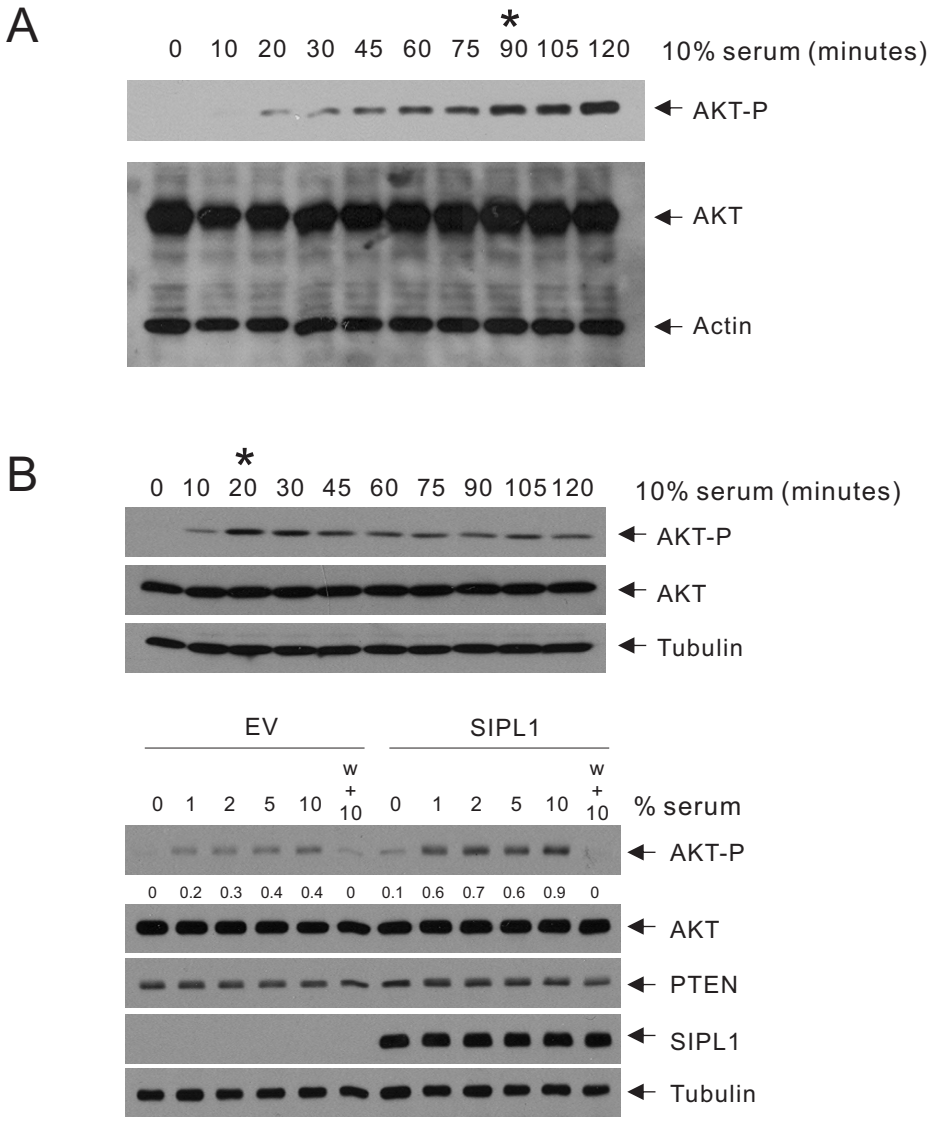

Supplementary Figure 5. SIPL1 sensitizes serum-induced AKT activation. (A) Determination of the kinetics of serum-induced AKT activation in DU145 cells. DU145 cells were serum starved for 6 hours and then stimulated with 10% serum for the indicated duration, followed by examination for AKT-P, total Akt, and Actin. * indicates the time-point, at which serum induced a plateau level of AKT activation. (B) MCF7 cells were serum-starved for 6 hours, followed by stimulation with 10% serum for the indicated duration and then examination for AKT activation (AKT-P), total AKT, and tubulin by western blot. * indicates the time-point at which a plateau level of AKT activation was achieved. All panels were derived from the same membrane (top panel). MCF7 cells were stably infected with empty vector (EV) or SIPL1 retrovirus, followed by serum starvation and induction of AKT activation for 20 minutes with the indicated doses of serum. The expression of AKT-P, total AKT, PTEN, SIPL1, and tubulin was determined by western blot using specific antibodies. All panels were derived from the same membrane (bottom panel). AKT-P was quantified by first normalizing AKT against the respective tubulin and then normalizing AKT-P against the normalized total AKT. Levels of AKT-P were presented under the AKT-P panel (bottom panel). Quantification of AKT-P was performed using the Scion Image software on scanned western blot images. Experiments were repeated once and typical results were presented.

Supplementary Figure 6

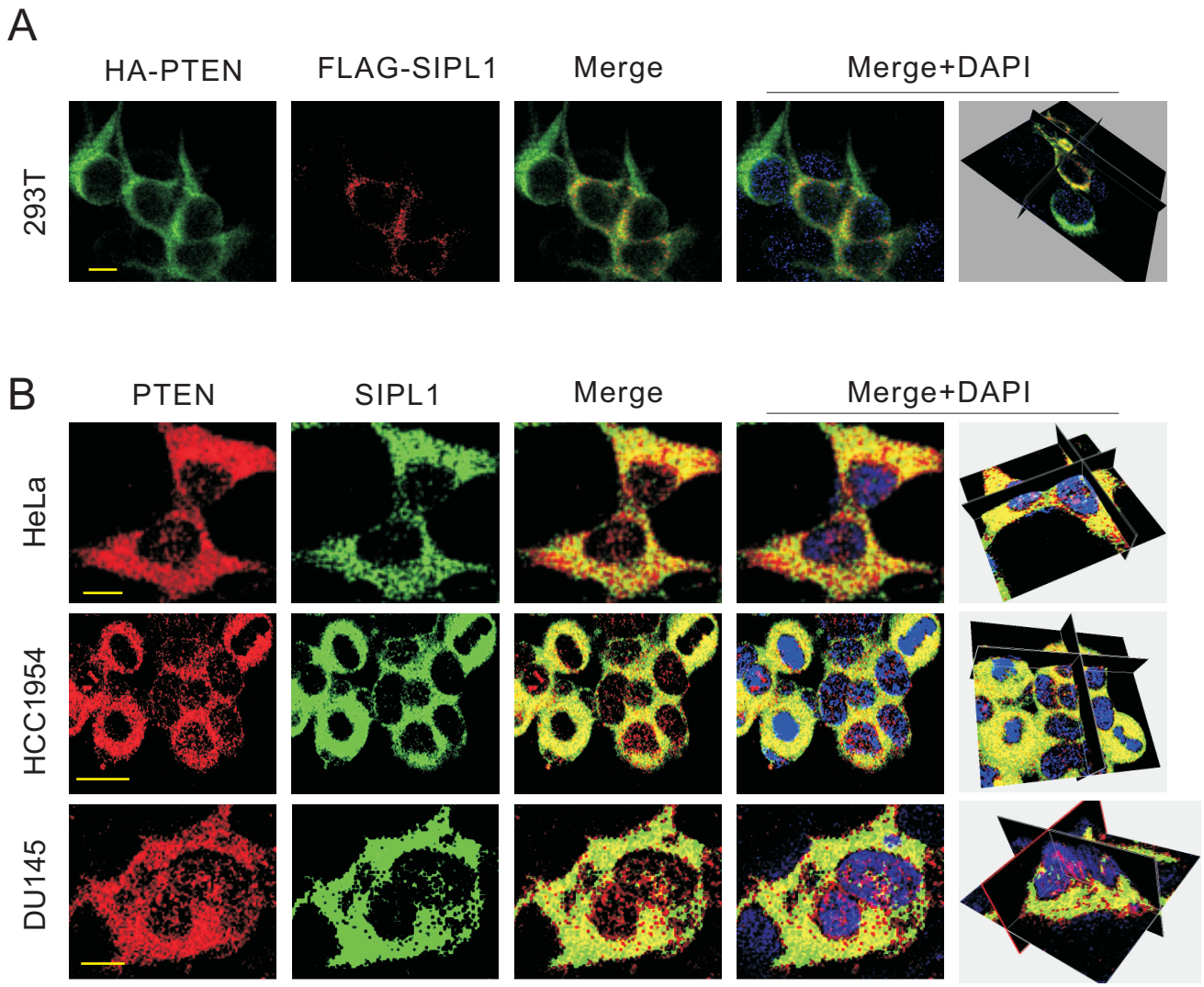

Supplementary Figure 6. PTEN co-localizes with SIPL1 in the cell. Ectopic PTEN and ectopic SIPL1 (A) and their endogenous counterparts (B) in the indicated cells were double IF stained. Nuclei were counter-stained with DAPI (blue). A set of z-stack images were taken using a MP Leica TCS SP5 confocal microscope. Images were analyzed and 3-D images were re-constructed using the IMARIS software. Typical z-stack images (left four panels) and 3-D images (right panel) are shown. Scale bars: 10 μm.

Supplementary Figure 7

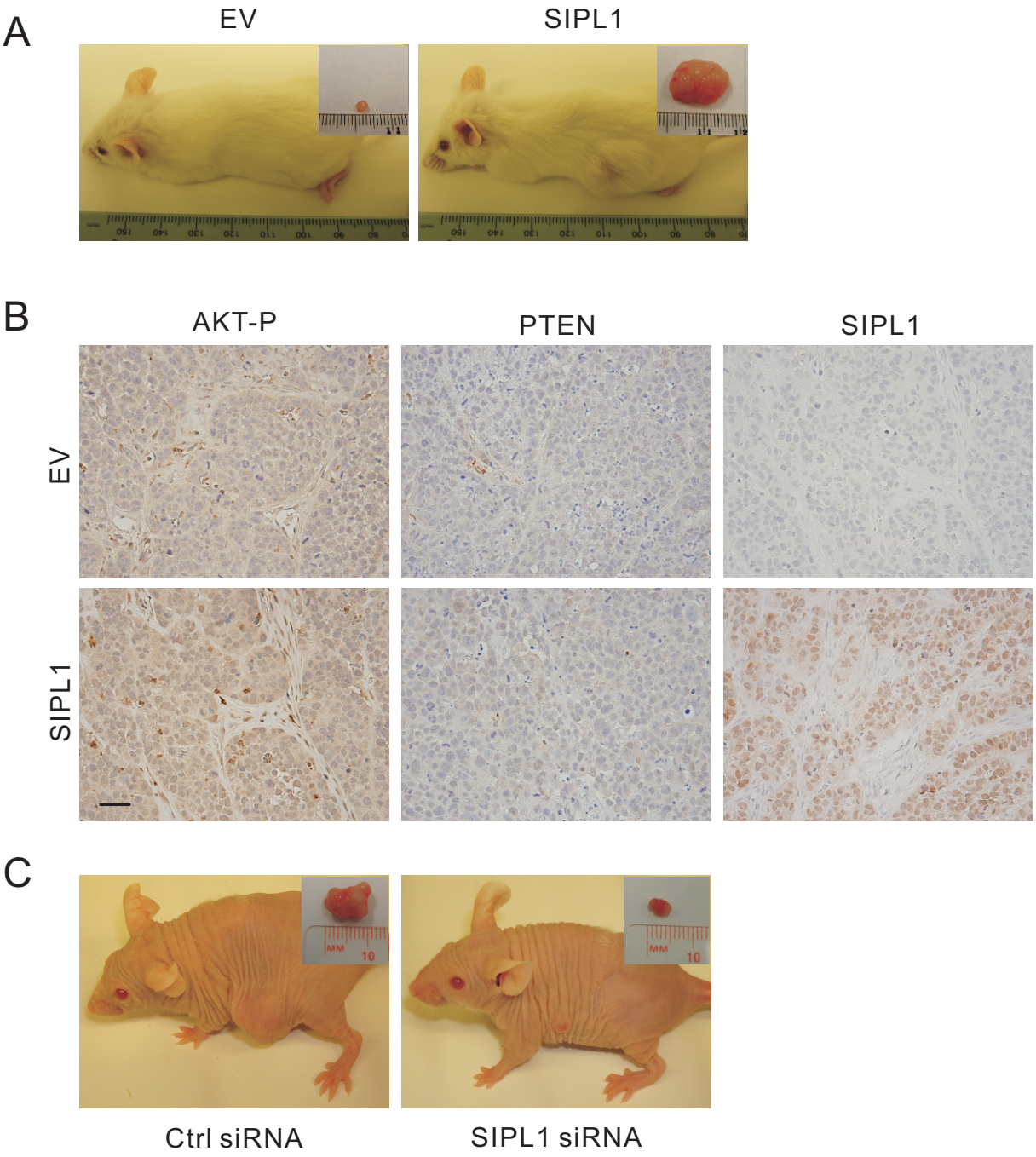

Supplementary Figure 7. SIPL1 promotes xenograft tumor formation via inhibiting PTEN function. HeLa cells were infected with the indicated retrovirus. Expression of ectopic SIPL1 was confirmed (see Figure 8). 10^6 cells were s.c. implanted into NOD/SCID mice (5 mice per group). Typical tumors were shown (**A**) and were IHC examined for AKT-P, PTEN, and SIPL1 (using anti-FLAG antibody, M2) (**B**). (**C**) $6x10^6$ HeLa cells were s.c. implanted into nude mice. At day 7, mice were randomly divided into 2-groups (5 mice per group) to receive either Ctrl siRNA or SIPL1 siRNA using **AteloGene.** Typical tumors at day 18 after delivery of siRNA are shown. Experiments were repeated once. EV: empty vector. Scale bar: 50 μm.

Supplementary Figure 8

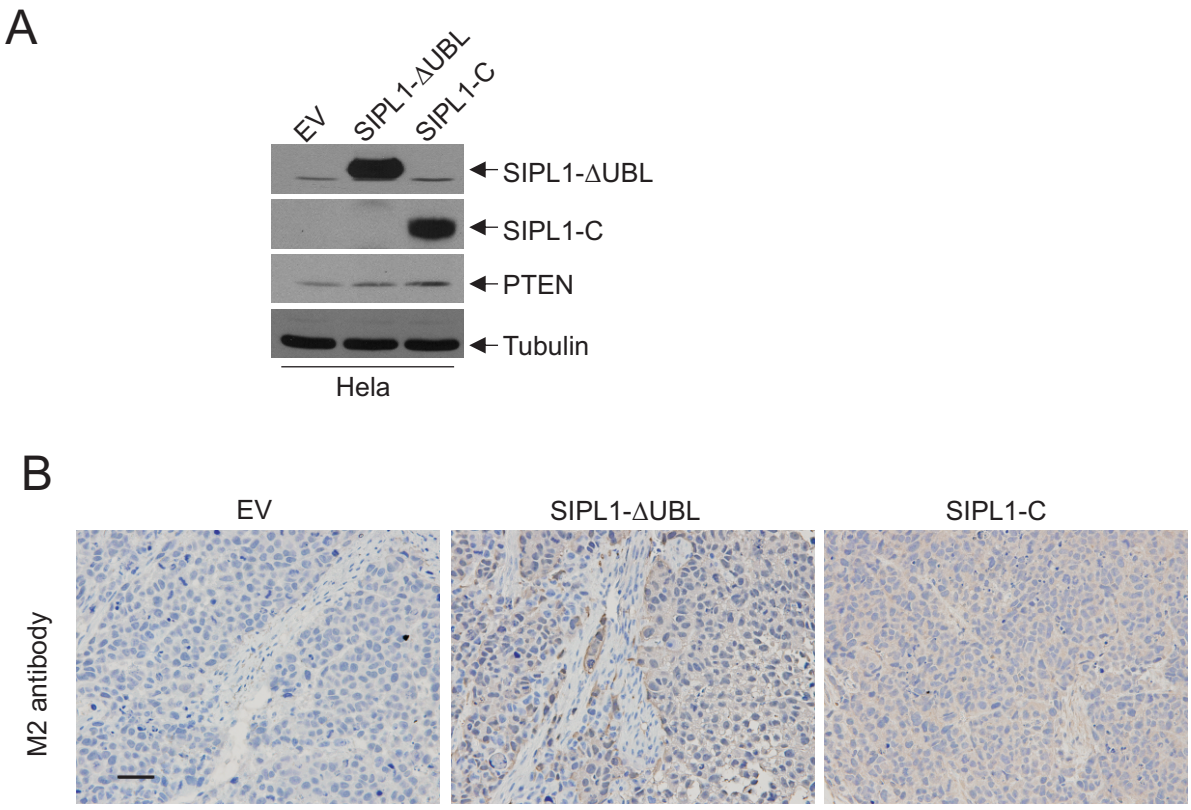

Supplementary Figure 8. Generation of xenograft tumors using HeLa cells stably expressing SIPL1 mutants. HeLa cells were stably infected with EV, SILP1-ΔUBL, or SIPL1-C retrovirus. These cells were then implanted into NOD/SCID mice (5 mice/cell lines). Xenograft tumor data were presented in Supplementary Table 1. In comparison to EV, overexpression of SILP1-ΔUBL and SIPL1-C did not enhance the formation of xenograft tumors (Supplementary Table 1). Expression of ectopic SILP1-ΔUBL and SIPL1-C in individual stable cell lines (**A**) and in the respective xenograft tumors determined by IHC using M2 anti-FLAG antibody (**B**) was demonstrated. Control IgG did not produce detectable signal (data not shown). Scale bar: 50 μm.

Supplementary Figure 9

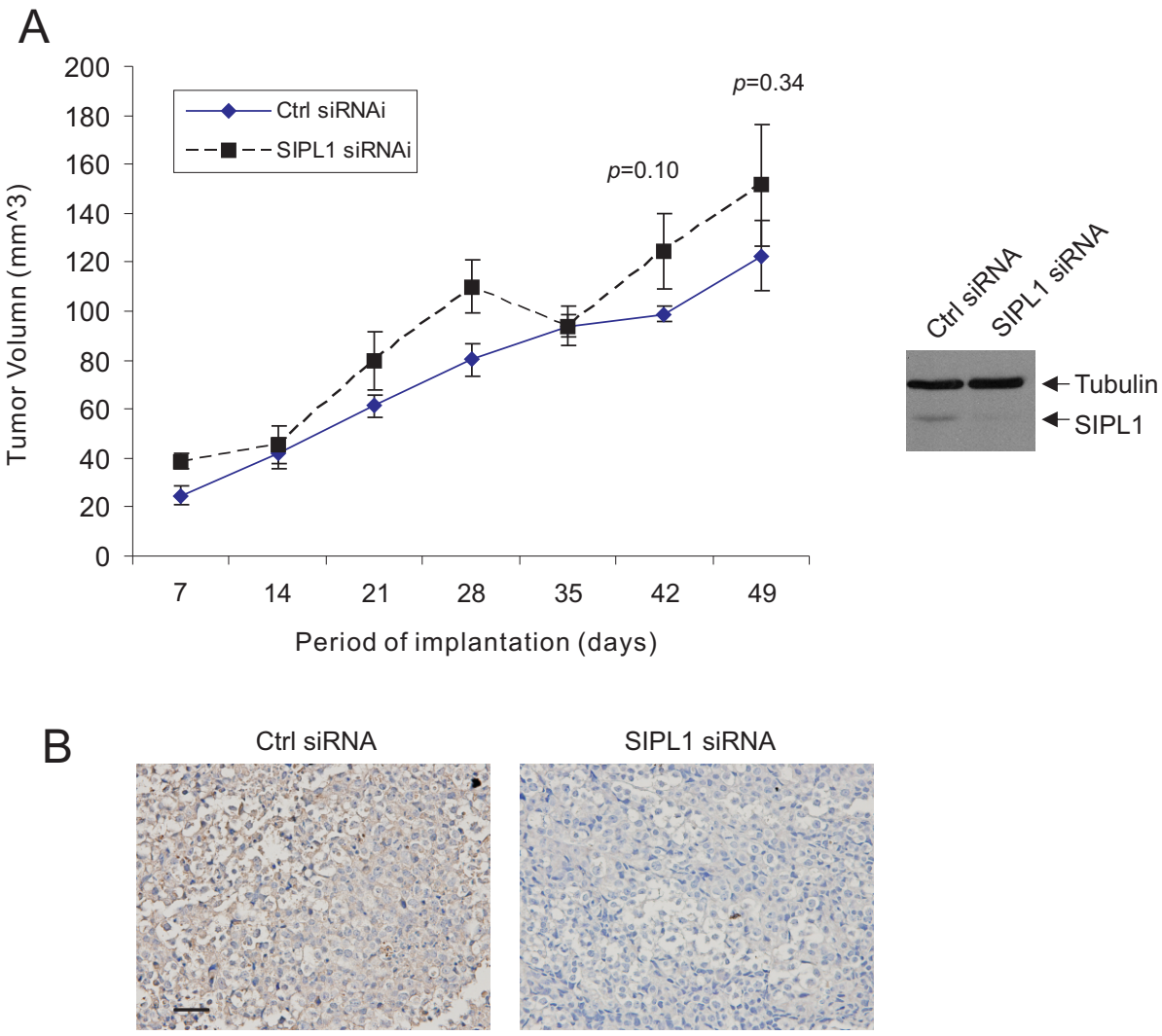

Supplementary Figure 9. Knockdown of SIPL1 does not affect the formation of PTEN deficient C33A cells-derived xenograft tumors. (**A**) C33A cells were treated with retrovirus expressing a Ctrl siRNA or PTEN siRNA. Knockdown of SIPL1 was demonstrated by western blot (right panel). 10^6 cells were implanted into NOD/SCID mice (1 implantation/mouse, 5 mice per cell line). Tumor incidence was 5/5 (number of tumors formed/number of implantations) for both cell lines (data not shown). Tumor volumes were monitored weekly. No significant difference was observed between xenograft tumors formed by Ctrl siRNA and SIPL1 siRNA ($p > 0.05$). (**B**) Xenograft tumors were IHC stained using anti-SIPL1 antibody. Control IgG did not produce detectable signals (data not shown). Scale bar: 50 μm.

Supplementary Figure 10

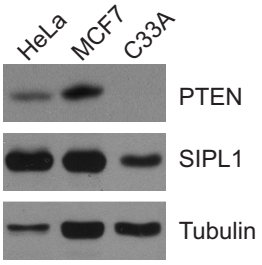

Supplementary Figure 10. C33A cells are PTEN negative. Western blot examination of PTEN, SIPL1, and tubulin expression in HeLa, MCF7, and C33A cells.

Supplementary Table 1. SIPL1 mutants do not enhance formation of HeLa cells-derived xenograft tumors.

Days [1]	Cell lines [2]	Tumor volume (mm^3) Mean±SEM	Tumor incidence [3]	Kruskal Wallis Statistics Test
7	EV	44.43±5.26	5/5	$p = 0.990$
	SIPL1-ΔUBL	48.96±6.91	5/5	
	SIPL1-C	43.25±5.57	5/5	
14	EV	28.88±2.12	5/5	$p = 0.403$
	SIPL1-ΔUBL	32.78±7.45	5/5	
	SIPL1-C	43.12±8.52	5/5	
21	EV	91.99±14.15	5/5	$p = 0.229$
	SIPL1-ΔUBL	69.63±6.50	5/5	
	SIPL1-C	68.87±9.55	5/5	
28	EV	329.05±60.05	5/5	$p = 0.137$
	SIPL1-ΔUBL	257.57±57.65	5/5	
	SIPL1-C	191.14±63.57	5/5	
35	EV	453.90±102.52	5/5	$p = 0.196$
	SIPL1-ΔUBL	360.45±112.04	5/5	
	SIPL1-C	217.92±80.10	5/5	
39	EV	487.70±101.73	5/5	$p = 0.379$
	SIPL1-ΔUBL	367.92±81.45	5/5	
	SIPL1-C	341.73±157.17	5/5	

[1] Days after tumor implantation.

[2] HeLa cells were stably infected with the indicated retrovirus and 2 x 10^6 cells were s.c. implanted into the left flanks of NOD/SCID mice.

[3] Number of xenograft tumors formed/number of implantations.

SEM: standard error of mean

Supplementary Table 2. SIPL1 promotes xenograft tumor formation via inhibiting PTEN function.

Days [1]	siRNA treatments [2]	Tumor volume (mm^3) Mean±SEM	Tumor incidences [3]	*t*-test [4]
21	Ctrl siRNA	45.12±8.62	5/5	0.017*
	PTEN siRNA	107.85±19.00	5/5	
	SIPL1 siRNA	47.28±6.07	5/5	0.058
	PTEN siRNA+SIPL1 siRNA	67.78±7.01	5/5	
28	Ctrl siRNA	57.31±29.44	5/5	0.038*
	PTEN siRNA	215.99±56.53	5/5	
	SIPL1 siRNA	51.11±5.59	5/5	0.018*
	PTEN siRNA+SIPL1 siRNA	100.84±15.75	5/5	
35	Ctrl siRNA	158.04±54.25	5/5	0.068
	PTEN siRNA	422.39±112.77	5/5	
	SIPL1 siRNA	86.42±8.15	5/5	0.052
	PTEN siRNA+SIPL1 siRNA	176.47±38.56	5/5	
42	Ctrl siRNA	265.68±82.26	5/5	0.091
	PTEN siRNA	656.19±186.23	5/5	
	SIPL1 siRNA	96.68±16.04	5/5	0.034*
	PTEN siRNA+SIPL1 siRNA	261.55±62.51	5/5	

[1] Days after tumor implantation.

[2] HeLa cells were infected with the indicated retrovirus. 1.5×10^5 individual cells were s.c. implanted.

[3] Number of xenograft tumors formed/number of implantations. Five NOD/SCID mice were used for each siRNA treatment.

[4] Two-tailed student *t* test. Statistical significance (*) is defined as $p < 0.05$.

SEM: standard error of mean

Supplementary Table 3. Patient's clinical information.

Patients	Pathology diagnosis	Age	Grade	TNM
1	Squamous cell carcinoma	45	1	T1N0M0
2	Squamous cell carcinoma	43	1	T1N1M0
3	Squamous cell carcinoma	58	1	T2aN0M0
4	Squamous cell carcinoma	55	1	T1N0M0
5	Squamous cell carcinoma	53	2	T2aN0M0
6	Squamous cell carcinoma	40	2	T1a1N0M0
7	Squamous cell carcinoma	47	1	T2bN0M0
8	Squamous cell carcinoma	40	1	T3aN0M0
9	Squamous cell carcinoma	49	1	T1N0M0
10	Squamous cell carcinoma (smooth muscle)	42	-	T1N0M0
11	Squamous cell carcinoma	48	2	T1bN0M0
12	Squamous cell carcinoma	44	2	T3N1M0
13	Squamous cell carcinoma	33	2	T1N0M0
14	Squamous cell carcinoma	43	2	T1N0M0
15	Squamous cell carcinoma	53	2	T2N1M0
16	Squamous cell carcinoma	55	2	T1N0M0
17	Squamous cell carcinoma	37	2	T3N0M0
18	Squamous cell carcinoma	43	2	T1N0M0
19	Squamous cell carcinoma	52	1	T1b1N1M0
20	Squamous cell carcinoma (chronic inflammation of smooth muscle)	36	-	T1b1N0M0
21	Squamous cell carcinoma (sparse)	40	-	T1N0M0
22	Squamous cell carcinoma	53	2	T2aN1M0
23	Squamous cell carcinoma	39	2	T1a1N0M0
24	Squamous cell carcinoma	49	2	T2N0M0
25	Squamous cell carcinoma	42	1	T2bN0M0
26	Squamous cell carcinoma (chronic inflammation of cervical canals)	70	-	T2bN0M0
27	Squamous cell carcinoma (cataplasis)	37	-	T1N0M0
28	Squamous cell carcinoma	50	2	T1N0M0
29	Squamous cell carcinoma	36	2	T3aNxM0
30	Squamous cell carcinoma	42	2–3	T1N0M0
31	Squamous cell carcinoma	42	2	T2bN0M0
32	Squamous cell carcinoma	70	2	T1N0M0

33	Squamous cell carcinoma	51	2	T2bN0M0
34	Squamous cell carcinoma	53	1	T1N0M0
35	Squamous cell carcinoma	42	2	T1N0M0
36	Squamous cell carcinoma	44	2	T1N0M0
37	Squamous cell carcinoma	47	2	T1N0M0
38	Squamous cell carcinoma	27	2	T1N1M0
39	Squamous cell carcinoma (sparse)	53	-	T2aN0M0
40	Squamous cell carcinoma (fibrous tissue and blood vessel)	40	-	T2bN0M0
41	Squamous cell carcinoma	43	2	T2bN0M0
42	Squamous cell carcinoma	41	3	T1b1N0M0
43	Squamous cell carcinoma	48	2	T1b1N0M0
44	Squamous cell carcinoma	58	2	T2aN0M0
45	Squamous cell carcinoma (smooth muscle and blood vessel)	46	-	T1aN0M0
46	Squamous cell carcinoma	29	2	T2aN0M0
47	Squamous cell carcinoma	39	2	T1N0M0
48	Squamous cell carcinoma	53	2	T1bN0M0
49	Squamous cell carcinoma	48	2	T2aN0M0
50	Squamous cell carcinoma	51	3	T2bN1M0
51	Squamous cell carcinoma	43	2	T2bN0M0
52	Squamous cell carcinoma	42	2	T1N0M0
53	Squamous cell carcinoma	52	2	T1N0M0
54	Squamous cell carcinoma	49	2	TxNxMx
55	Squamous cell carcinoma	36	2	T2bN0M0
56	Squamous cell carcinoma	46	2	-
57	Squamous cell carcinoma	36	2	T2aN0M0
58	Squamous cell carcinoma	45	2	T2aN0M0
59	Squamous cell carcinoma	42	2	T2N1M0
60	Squamous cell carcinoma	52	2	T2aN0M0
61	Squamous cell carcinoma	40	2	TxN0M0
62	Squamous cell carcinoma	45	2	T2N1M0
63	Squamous cell carcinoma	62	2–3	T2N1M1
64	Squamous cell carcinoma	44	2	T2aN0M0
65	Squamous cell carcinoma	35	2	T1a2N0M0
66	Squamous cell carcinoma	36	2	T1bN0M0
67	Squamous cell carcinoma	42	2–3	T2aN0M0

68	Squamous cell carcinoma	47	3	T2bN0M0
69	Squamous cell carcinoma	39	3	T1b2N0M0
70	Squamous cell carcinoma	43	3	T1a2N1M0
71	Squamous cell carcinoma	53	2	T1bN0M0
72	Squamous cell carcinoma	54	2	T2aN0M0
73	Squamous cell carcinoma	39	2	T1N1M0
74	Squamous cell carcinoma	36	2	T2bN0M0
75	Squamous cell carcinoma	30	3	T2bN1M0
76	Squamous cell carcinoma	55	3	T1a2N0M0
77	Squamous cell carcinoma	53	3	T2aN0M0
78	Squamous cell carcinoma	26	3	T2N0M0
79	Squamous cell carcinoma	53	3	T2N0M0
80	Squamous cell carcinoma	37	3	T1N1M0
81	Squamous cell carcinoma	41	3	T1b1N1M0
82	Adenosquamous carcinoma	48	-	T1b2N1M0
83	Squamous cell carcinoma	39	3	T2aN0M0
84	Squamous cell carcinoma	41	3	T1N0M0
85	Squamous cell carcinoma	53	3	T1b1N0M0
86	Endocervical-type mucinous adenocarcinoma	50	1	T1N0M0
87	Enteric-type adenocarcinoma	43	2	T1b2N0M0
88	Endometrioid-type adenocarcinoma	32	2	T1a1N0M0
89	Clear-cell type adenocarcinoma	40	2	T1aN0M0
90	Endocervical-type mucinous adenocarcinoma	50	2–3	TxN1M0
91	Enteric-type adenocarcinoma	51	3	T1aN0M0
92	Adenocarcinoma	52	2–3	T1bN0M0
93	Serous papillary adenocarcinoma	44	1	T1aN0M0
94	Carcinoma sarcomatodes	51	-	T1b2N0M0
95	Cancer adjacent normal cervical tissue	47	-	-
96	Cancer adjacent normal cervical tissue	41	-	-
97	Cancer adjacent normal cervical tissue (fibrous tissue and blood vessel)	43	-	-
98	Cancer adjacent normal cervical tissue	40	-	-
99	Cancer adjacent normal cervical tissue	43	-	-
100	Normal cervical tissue	18	-	-
101	Normal cervical canals tissue	40	-	-
102	Normal cervical tissue	21	-	-

103	Normal cervical tissue	15	-	-
104	Normal cervical tissue	21	-	-
105	Malignant melanoma (tissue marker)	58	-	